RC23794 (W0511-084) November 10, 2005
Materials Science

IBM Research Report

Interfacial Microstructure of NiSix/HfO_2/SiOx/Si Gate Stacks

M. A. Gribelyuk
IBM Semiconductor Research and Development Center (SRDC)
Systems and Technology Group
Hopewell Junction, NY 12533

C. Cabral Jr., E. P. Gusev, V. Narayanan
IBM Semiconductor Research and Development Center (SRDC)
IBM Research Division
Thomas J. Watson Research Center
P.O. Box 218
Yorktown Heights, NY 10598

Research Division
Almaden - Austin - Beijing - Haifa - India - T. J. Watson - Tokyo - Zurich

LIMITED DISTRIBUTION NOTICE: This report has been submitted for publication outside of IBM and will probably be copyrighted if accepted for publication. It has been issued as a Research Report for early dissemination of its contents. In view of the transfer of copyright to the outside publisher, its distribution outside of IBM prior to publication should be limited to peer communications and specific requests. After outside publication, requests should be filled only by reprints or legally obtained copies of the article (e.g., payment of royalties). Copies may be requested from IBM T. J. Watson Research Center , P. O. Box 218, Yorktown Heights, NY 10598 USA (email: reports@us.ibm.com). Some reports are available on the internet at http://domino.watson.ibm.com/library/CyberDig.nsf/home.

Interfacial microstructure of NiSix/HfO_2/SiOx/Si gate stacks

M. A. Gribelyuk[1], C. Cabral Jr.[2], E. P. Gusev[2], V. Narayanan[2]

IBM Semiconductor Research and Development Center (SRDC)

[1] Systems and Technology Group, Hopewell Junction, NY 12533

[2] T J Watson Research Center Yorktown Heights NY 10598

Abstract

Integration of NiSix based fully silicided (FUSI) metal gates with HfO_2 high-k gate dielectrics offers promise for further scaling of complementary metal-oxide-semiconductor (CMOS) devices. A combination of High Resolution TEM (HRTEM) and small probe electron energy loss spectroscopy (EELS) and energy dispersive x-ray (EDX) analysis has been applied to study interfacial reactions in the undoped gate stack. NiSi was found to be polycrystalline with the grain size decreasing from top to bottom of NiSix film. Ni content varies near the NiSi/HfOx interface whereby both Ni-rich and monosilicide phases were observed. Spatially Non-uniform distribution of oxygen along NiSix/HfO_2 interface was observed by dark field STEM imaging and EELS. Interfacial roughness of NiSix/HfOx was found higher than that of poly-Si/HfO_2, likely due to compositional non-uniformity of NiSix. No intermixing between Hf, Ni and Si beyond interfacial roughness was observed.

Introduction

Decreases in device dimensions, or device scaling, has lead to a continuous increase in device speed and reduction of cost in production over a number of generations of CMOS technology. One of the ways to increase device speed involves increasing gate capacitance, which has been accomplished by scaling the thickness of the gate oxide. Silicon oxynitrides are used as gate dielectrics largely because they can be easily integrated into semiconductor process flow. The leakage current caused by direct tunneling of charge carriers from the gate to the channel region of a device increases exponentially with decreasing the gate oxide thickness. This sets the limit for scaling of gate oxides, otherwise they can not be implemented in low power circuits. Gate oxide reliability as well as boron penetration in p-fet devices present other problems caused by scaling of a gate oxide thickness.

For the last 10 years many efforts have been put into replacement of silicon oxyinitride by the one with higher dielectric constant, i.e. high-k oxide, which would allow one to achieve the same device speed with the thicker gate dielectric, and thus continue scaling its thickness without significantly increasing leakage current. One possibility is to replace the gate dielectric alone and keep poly-Si as the metal-oxide-semiconductor field effect (MOSFET) device gate. Control of charge both inside the high-k dielectric and at its interfaces with Si and poly-Si along with the observed reduction of carrier mobility present some of the challenges of this scheme. In particular, large shifts of threshold voltage in a p-FET device with Hf oxide gate dielectric (as compared to the one with Si oxynitride) has made realization of a p-FET device difficult [1].

The other option includes replacement of poly-Si with metal gate together with the dielectric. It eliminates depletion in heavily doped poly-Si gates, thus reducing electrical thickness of gate dielectric. Since doping is not necessary to make the gate conductive there is no boron penetration effect from gate into channel region of device in p-FET devices. For CMOS technology this would require two types of metals with respective work functions, i.e. for n-FET and p-FET devices. The challenge is the integration placement of two different gate materials into CMOS process flow. An attractive option

to solve this problem includes silicidation of poly-Si to convert it to metal and adjustment of its work function for n-fet and p-fet devices by doping. The first detailed review of properties of various refractive metals for application as low resistivity contacts in integrated circuits and fully silicided gates (FUSI) dates back to 1980 [2]. Recent work on NiSix FUSI showed that a NiSi monosilicide gate has a midgap work function [3], which can be adjusted by doping with As, P, Sb [4] for n-FET and B (5) or using Ni(Pt)S silicide with Al predoped poly-Si [6] for the p-fet. The gate leakage reduction in 6 to 7 orders of magnitude was reported in devices based on FUSI/$HfSiO_x$ stacks. [7]. These devices also showed improved drive current at the gate dielectric thickness Tinv= 2nm measured in the inversion regime from C-V device characteristics.

It is important to understand and control interfacial reactions and composition in the gate stack. Indeed, the work function of a NiSi gate was found dependent on the phase of NiSix [8]. We report on intermixing and microstructure of an undoped NiSi/HfO_2/SiOx/Si gate stack using a combination of high resolution and analytical TEM. Interfacial roughness of NiSi/HfO_2 interface is compared to that of poly-Si/HfO_2. Composition and phase uniformity of NiSix gate is analyzed, as it is important for control of its work function.

Experimental

A n-doped Si substrate capped with a 9Å thick Si oxide was used. A 3nm thick Hf oxide film was grown by metallo-organic chemical vapor deposition (MOCVD). After poly-Si and Ni were deposited by low pressure chemical vapor deposition (LPCVD) and physical vapor deposition (PVD), correspondingly, the stack was annealed at T= 450^0C for t=50s in the nitrogen ambient to form Ni silicide. x-sectional samples for TEM analysis were prepared by mechanical polishing. Final thinning of the samples was done by Ar ion milling until electron transparency. A JEOL-2010F TEM with the point-to-point spatial resolution d= 1.9Å was used for conventional and high-resolution transmission electron microscopy. EDX and electron energy loss spectroscopy (EELS) analysis were performed in STEM mode using ESvision acquisition system. The small focused probes of a size 5Å and 7Å were used.

Results

The overall microstructure of a gate stack is shown in Fig. 1. The top part of $NiSi_x$ has columnar grain structure with the grain size up to 50nm. The Cr overlayer was deposited on to NiSix during TEM sample preparation. We found that composition of the $NiSi_x$ film is not uniform. First, let us consider evidence from EDX analysis (Fig. 2). Fig. 2a shows a dark field STEM image of a NiSi film formed by a 7 Å small electron probe. A series of EDX spectra was taken along the line shown in Fig.2a. Ni $K\alpha_1$ and Si $K\alpha_1$ lines were quantified using a mixed model with no thickness correction. Fig.2b shows variation of atomic fraction of Ni in NiSix from a top part of the film to the bottom. No other species except for Ni and Si were detected by EDX. We find that the top portion of NiSix is Ni rich while the Ni:Si ratio is 1 at the bottom of the film. If approximated by a linear fit the atomic fraction varies at a rate 0.01/nm in the depth direction of a $NiSi_x$ film. It should be noted that the decrease of the Ni fraction toward the bottom of a film is in agreement with the silicidation mechanism whereby a monosilicide phase NiSi is formed by diffusion of Ni atoms into Si from a Ni film deposited on top of poly-Si [9]. The Ni was deposited in excess such that when all the poly-Si is consumed the remaining Ni not in the NiSi phase remains at the top of the film in the metal rich phase. The phase formation sequence goes from Ni_3Si, $Ni_{31}Si_{12}$, Ni_2Si, Ni_3Si_2, NiSi and then $NiSi_2$ and will stop once all the poly-Si is consumed.

EDX data in Fig. 2 was collected from a region of a TEM sample which is thicker than the grain size. In this case the EDX data will represent the average over few grains in the direction of electron beam and thus will not be able to provide phase information. Therefore we turn to high resolution TEM (Fig. 3) to determine the phase of NiSix. We find small grains at the bottom of a film, as opposed to large grains found in its top part (Fig. 1). The small grain size near NiSix/HfO_2 interface confirms that EDX data is not adequate for phase determination at the bottom of a NiSix film. In Fig. 3 some grains are imaged as bright regions as opposed to darker grains around them. In the imaging conditions used the brighter the grain the less is the Ni content in it. This suggests, that composition of NiSix grains varies from grain to grain. Lastly, we determine the phase of

an individual grain by matching its lattice parameters measured from the lattice image with those of NiSix structures determined from x-ray analysis.

The crystalline grain of NSi_x has the following lattice parameters: d_1= 2.18Å, d_2= 1.98Å with the angle between respective lattice planes α= 80.7^0. The best match for the orthorhombic nickel monosilicide phase NiSi [10] is achieved, if one assumes that spacings d_1 and d_2 correspond to (120) and (021) crystal planes with spacings $d_{(120)}$= 2.35 Å, $d_{(021)}$= 2.04 Å and the angle α= 44^0 between them. Clearly the difference between the measured and theoretical data is larger than experimental errors of measuring interplaner distances and the angle between them. Thus, the match is not satisfactory. Experimental data was compared to a number of Ni-rich silicide phases and the best match for each phase is listed in Table 1. We found that the monoclinic Ni_3Si structure [14] with lattice spacings $d_{(-311)}$ = 2.122 Å, $d_{(-222)}$= 1.96 Å and α= 79.3^0 offers the best match among all other $NiSi_x$ phases. The cubic Ni_3Si phase [15] is thermodynamically stable at temperatures T< 1035^{0}C according to Ni-Si phase diagram [16]. The monoclinic Ni_3Si is only stable at temperatures T> 990^{0}C, i.e. above silicidation reaction temperature T= 450^{0}C. The observation of the monoclinic Ni_3Si in the gate stack indicates that silicidation reaction has lead to formation of small Ni-Si precipitates of metastable phases. Variation of grain size from top to bottom of NiSix as well as observation of different phases near $NiSi_x/HfO_2$ interface prove that Ni diffusion during silicidation reaction and its final distribution is not uniform. The work function of NiSix FUSI gates depends on Ni content [8]. Therefore it is important to effectively control phase uniformity of NiSix to produce FUSI gate stacks with the fixed work function.

It should be noted, that the silicidation process has also led to increased roughness of NiSix/HfO_2 interface. Indeed, roughness up to 1nm is obvious from Fig.4a. It is natural to compare that to roughness of poly-Si/HfO_2 interfaces. We found from previous studies that interfacial roughness of poly-Si/HfO_2 depends on thickness of HfO_2 whereby the latter looses its continuity if its thickness is less than 2nm. Fig.4b shows that roughness of poly-Si/HfO_2 does not exceed 5Å if thickness of HfO_2 is 3nm, i.e. same thickness as of HfO_2 film in Fig.4a. In both cases of poly-Si/HfO_2 and NiSi/HfO_2 small grains are

observed near the interface with HfO_2. Therefore the grain size alone cannot explain the difference in roughness. We suggest that the higher interfacial roughness in Fig.4a is due to a non-uniform composition of NiSix grains at the bottom of NiSi film, as NiSix and HfO_2 films attempt to establish epitaxial relationship.

We will now consider compositional abruptness at the NiSix/HfOx interface. Fig. 5 shows elemental profiles of Hf and Ni as derived by EDX. In this experiment the electron beam of the size d= 7Å scans across the interface, and EDX spectrum is acquired at each position of the electron beam. Elemental profiles are derived by processing of EDX spectra, which are acquired at different beam positions. In Fig. 5 Hf Kα1 and Ni Kα1 peaks were utilized to profile distribution of Hf and Ni, respectively. It is evident that the overlap of both profiles does not exceed 2nm. It should be mentioned that activation volume for generation of characteristic x-rays is larger than the probe size. This leads to degradation of spatial resolution of EDX. Therefore the overlap of 2nm can be interpreted as effective spatial resolution of EDX rather than evidence of intermixing between Hf and Ni. Fig. 6 shows a dark field STEM image and respective elemental profiles for oxygen and Ni derived by EELS. Here a 5Å small electron probe was scanning along the line depicted in Fig.6a, and the EELS spectrum was acquired at each beam position. The oxygen K and Ni L3 edges were analyzed to profile distribution of oxygen and nikel. Oxygen K and Ni L3 edges arise at ΔE= 532ev and ΔE= 855eV in the EELS spectrum, respectively [17]. Position of interfaces in Fig. 6b was determined from a respective position of a beam in the STEM image (Fig. 6a). The contrast in the STEM image is qualitatively proportional to the atomic number of the scattering species. Therefore Hf oxide is imaged as the bright band and the interfacial layer between Si and Hf oxide is imaged as the dark band. Fig. 6b shows that Ni has not diffused into Hf oxide. This supports our conclusion that the observed overlap between Ni and Hf Kα1 x-ray peaks (Fig. 5) is caused by limited resolution of EDX, and not by intermixing.

On the other hand, an oxygen profile in Fig. 6b presents an interesting phenomenon. It shows that oxygen is present in the bottom part of NiSi, which is up to 2nm thick. The dark band between HfO_2 and NiSix in a respective STEM image (Fig 6a) also suggests,

that a light element is present at the interface. Two explanations can be suggested. First, oxygen could outdiffuse from Hf oxide; second, oxygen could have been introduced during Ni deposition and then piled up against Hf oxide during silicidation process. We will now prove that the second mechanism takes place. Fig. 7 shows elemental profiles for oxygen (O K edge) and Si (Si $L_{2,3}$ edge, ΔE= 99eV) in a gate stack S/SiOx/HfOx/poly-Si, which has undergone similar processing conditions except for silicidation reaction. It is evident that no oxygen is detected at the bottom of poly-Si. The slight offset in the oxygen profile is the same across the stack and is due to the background subtraction in the EELS spectrum. This suggests, that observation of oxygen at NiSix/HfO_2 interface is caused by a pile-up of oxygen during silicidation process, and is not due to outdiffusion of oxygen from Hf oxide. Its presence near the interface effectively changes a phase composition of NiSix. As judged from Fig. 6a oxygen distribution is not uniform along the interface. Both phenomena may affect work function of NiSix as well as lead to formation of charges at NiSix/HfO_2 interface. Therefore oxygen content should be controlled in the optimized NiSi FUSI gate stack.

Lastly, Fig. 8 presents EELS elemental profiles of Hf (M_5 edge, ΔE= 1662eV) and Si (K edge, ΔE= 1850eV) across NiSix/HfO_2 interface. The Hf M_5 edge was chosen rather than the Hf $O_{2,3}$ edge (ΔE= 31eV) to avoid interference between that edge and the Ni $M_{2,3}$ edge ((ΔE= 68eV) during background subtraction. These profiles were acquired in the same way as those in Figs.5-7. A 7Å small probe was used. They suggest that Hf is present in the bottom part of NiSi and Si is present in top and bottom portions of Hf oxide so that a 3nm thick Hf oxide turns in to (Si)HfOx/HfOx/(Si)HfOx. It should be noted, however, that NiSix/HfO_x and HfO_x/SiOx interfaces are rough up to 1nm, as evident from Fig. 4a. The typical TEM sample that is used for EELS analysis is few hundred Angstroms thick. An EELS signal is generated as a focused electron beam passes through a sample. If the interface is rough the beam passes through both adjacent layers as it transverses the sample near the interface. Therefore interfacial roughness blurs elemental profiles and can mimic intermixing. We cannot differentiate between intermixing and roughness in Fig. 8. However, extent of blurring in Fig. 8 is the same as roughness.

Therefore we suggest that it is mainly caused by interfacial roughness, and thus no intermixing between Hf and Si takes place.

Conclusions

The silicidation reaction has resulted in a composition gradient of NiSix whereby on the average some Ni-rich NiSix phases are formed at the top of a film. This finding is consistent with silicidation process taking place via Ni diffusion for the initially deposited Ni film. The bottom part of NiSix film produced under described conditions is found compositionally non-uniform and is comprised of small grains with varying phase content, including Ni-rich phases. Interfacial roughness of NiSi gate stacks was found higher than that of poly-Si stacks, which is attributed to compositional and crystallographic non-uniformity of NiSi in the bottom of a film. EELS and EDX small probe analysis have revealed that no intermixing takes place between NiSi and Hf oxide beyond interfacial roughness. The silicidation process has also led to some spatially non-uniform pile-up of oxygen in the bottom part of NiSi film. Since compositional non-uniformity near NiSix/HfO_2 interface affects device parameters it has to be strongly controlled in the optimized NiSi FUSI gate stack.

Acknowledgement

Authors are indebted to Dr. Matt Copel (IBM) for insightful discussions.

References

1. C. Hobbs, L. Fonseca, V. Dhandapani et. al. Symp. VLSI Tech. Dig.,2003
2. S. P. Murarka, J. Vac. Sci. Technol. , 1980, 17(4), p. 775
3. W. P. Maszara, Z. Krivokapic, P. King et. al. IEDM Tech Dig. , 2002 p.367
4. J. Kedzierski, D. Boyd, Z. Ying et. al., IEDM Tech Dig. , 2003 p.18.4.1
5. J. Kedzierski, E. Nowak, T. Kanarsky et. al., IEDM Tech Dig. , 2002 p.247
6. C. Cabral, J. Kedzierski, B. Linder et. al. VLSI Tech Dig.,2004 p. 184
7. E. Gusev, C. Cabral, Jr., B. P. Linder et. al. IEDM Tech Dig., 2004
8. M. Qin, V. M. C. Poon, S. C.H. Ho J. of Electrochem. Soc., 148 (5), p. G271 (2001)
9. J. E. E. Baglin et al., Thin Solid Films, **93**, p.255, 1982

10. Diffraction data, JCPDS file 85-0901 2000
11. Diffraction data JCPDS file 43- 0989 2000
12. Diffraction data JCPDS file 80-2283 2000
13. Diffraction data JCPDS file 03-1073 2000
14. Diffraction data, JCPDS file 32-0699 2000
15. Diffraction data, JCPDS file 06-0690 2000
16. Binary Alloy Phase Diagrams ed. by Th. B. Massalski, v. 2, p. 1755 (American Society for Metals, 1986).
17. C. C. Ahn, O.L. Krivanek, EELS Atlas (Gatan Inc.)

Table 1. Lattice parameters of different NiSix phases that provide the best match of lattice parameters derived from Fig. 3. Miller indexes of respective crystallographic planes are given in parenthesis.

Phase	**d_1, Å**	**d_2, Å**	**α, deg.**	**Reference**
	1.98	**2.12**	**80.7**	**This data**
orth.-NiSi	**1.98 (211)**	**2.046 (1-20)**	**90.0**	**[10]**
c-$NiSi_2$	**1.92 (220)**	**2.708 (002)**	**90.0**	**[11]**
hex- Ni_2Si	**1.96 (102)**	**2.44 (002)**		**[12]**
hex-Ni_5Si_2	**1.96 (204)**	**2.24 (212)**		**[13]**
m-Ni_3Si	**1.96 (-222)**	**2.12 (-311)**	**79.3**	**[14]**
c-Ni_3Si	**2.02 (111)**	**2.02 (1-11)**	**70.5**	**[15]**

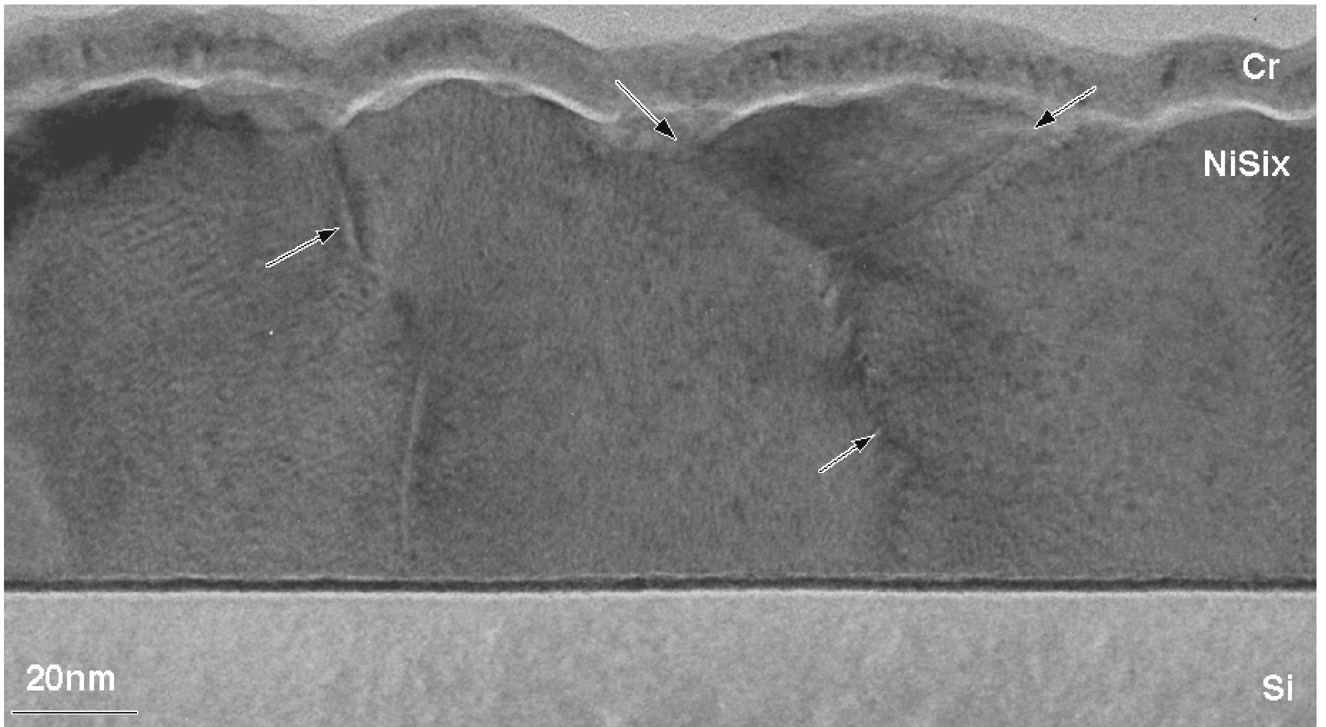

Fig. 1: Conventional TEM image of a FUSI gate stack. Individual NiSix grain boundaries are indicated with arrows.

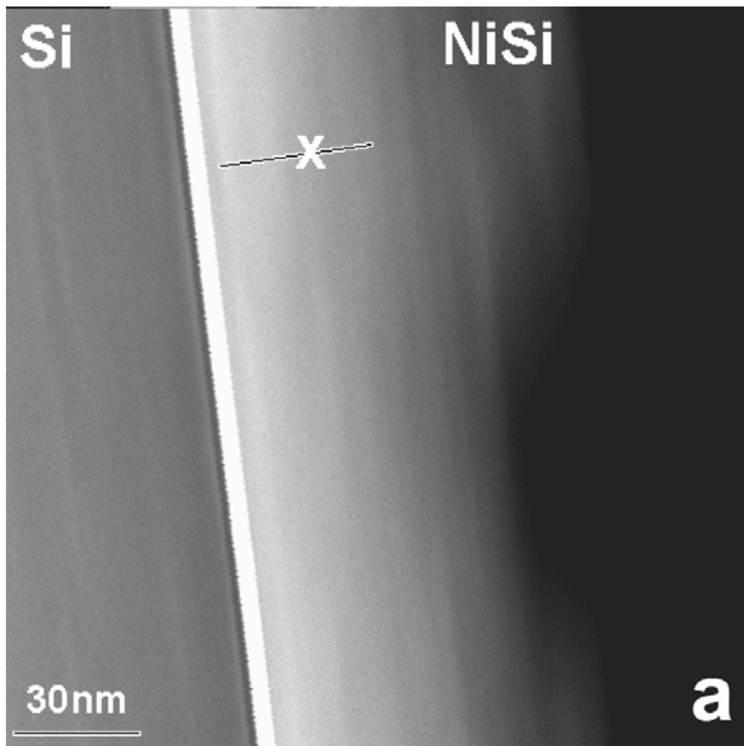

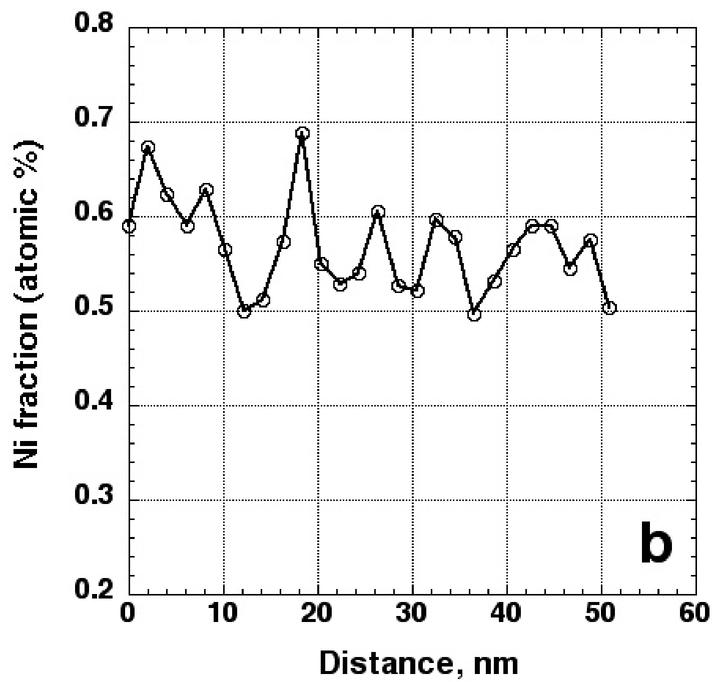

Fig.2: (a) Dark field STEM image. EDX spectra were taken at each point along profile in (a); (b) Depth dependence of atomic fraction of Ni. Origin corresponds to the top part of NiSix film.

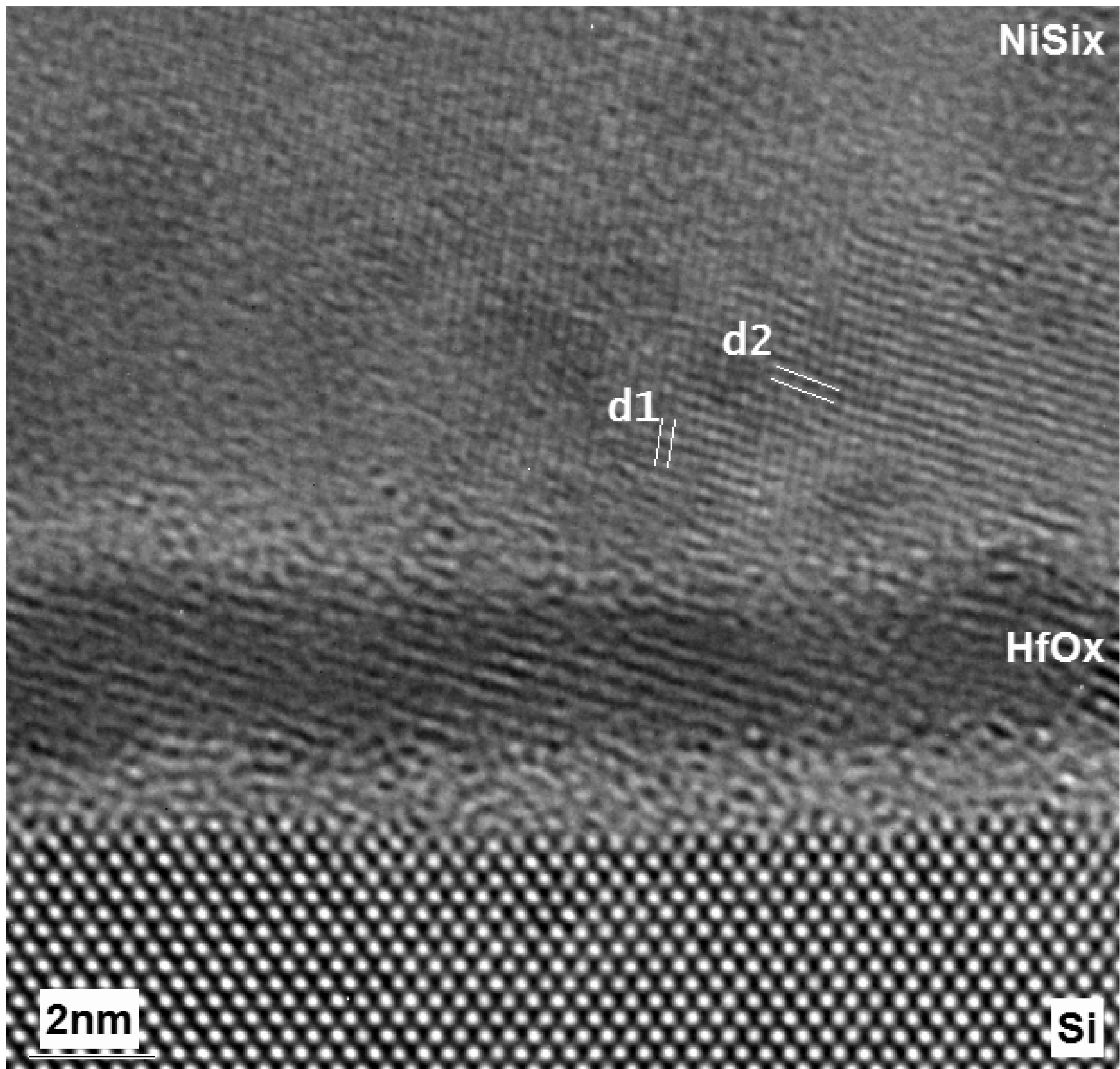

Fig.3: HRTEM image of NiSix/HfO_2 interface. An individual $NiSi_x$ grain with measured lattice parameters is labeled. Bright region next to HfO_2 is attributed to presence of oxygen. Variation of pattern in SiSix is caused by a different extent of silicidation.

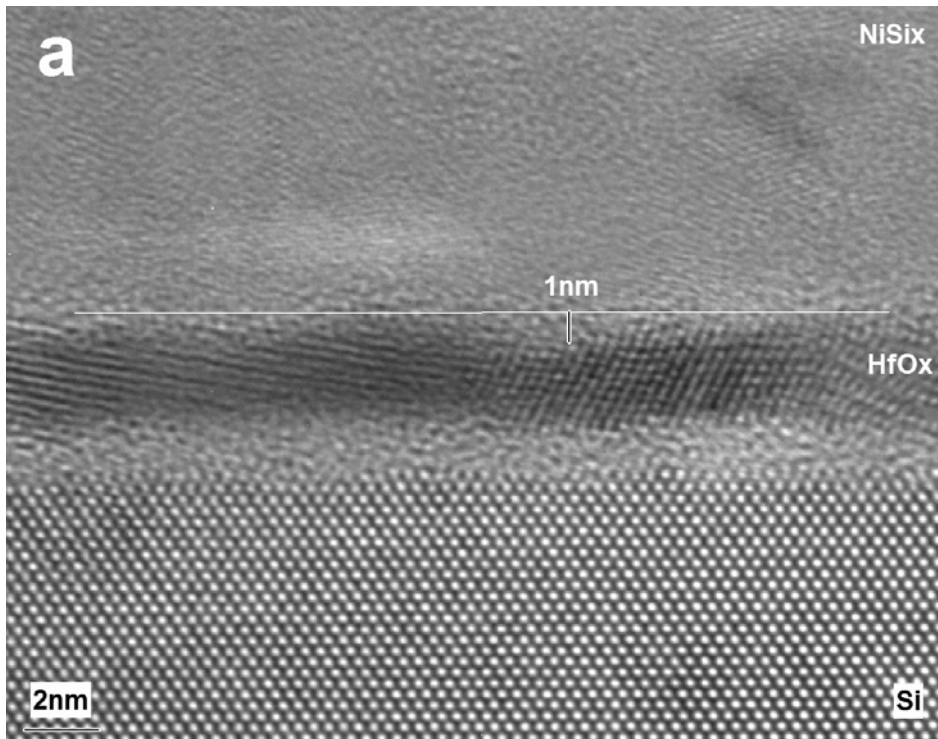

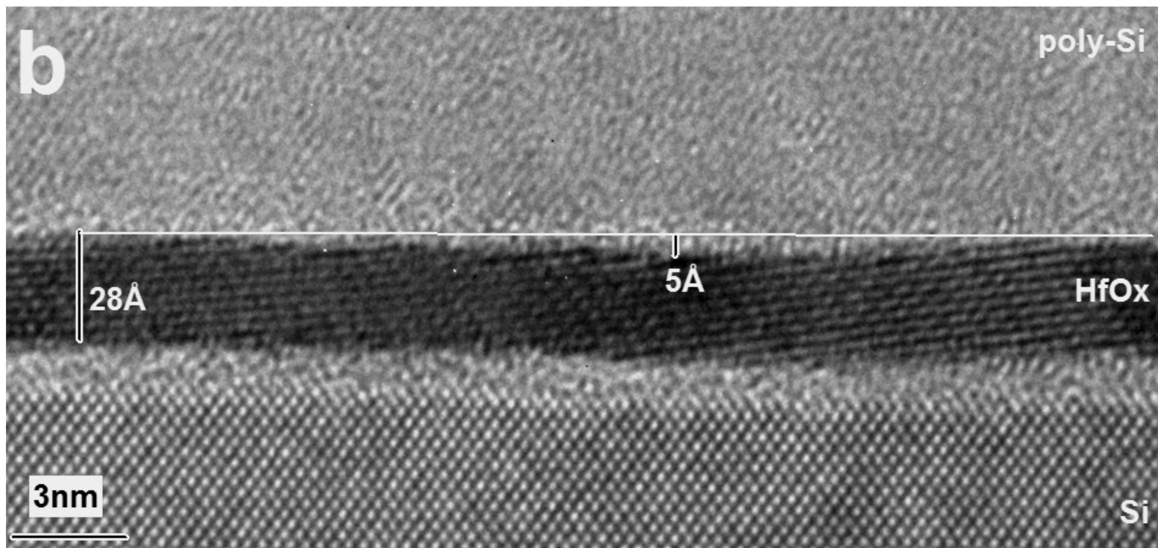

Fig. 4: Interfacial roughness of a FUSI/HfOx/SiOx/Si gate stack (a) and as-deposited poly-Si gate stack with same gate dielectric (b). SiOx/HfO_2 roughness is comparable. Roughness of NiSix/HfO_2 is higher than that of poly-Si/HfO_2.

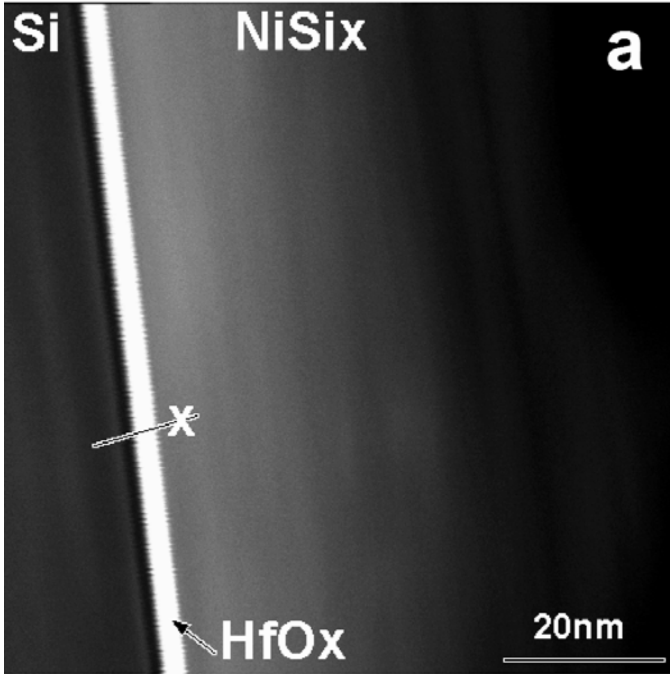

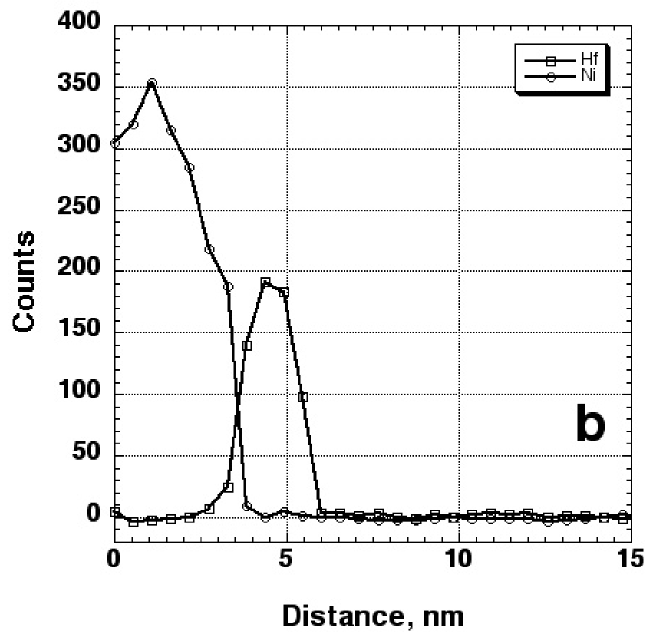

Fig. 5: (a) Dark field STEM image of FUSI gate stack. EDX spectra were taken at each point along profile in (a); (b) Elemental profiles of Ni (open circles) and Hf (open squares).

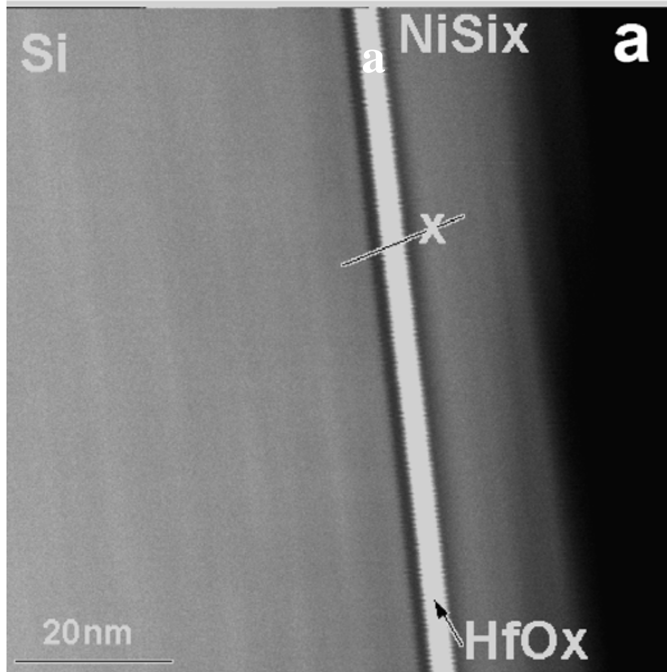

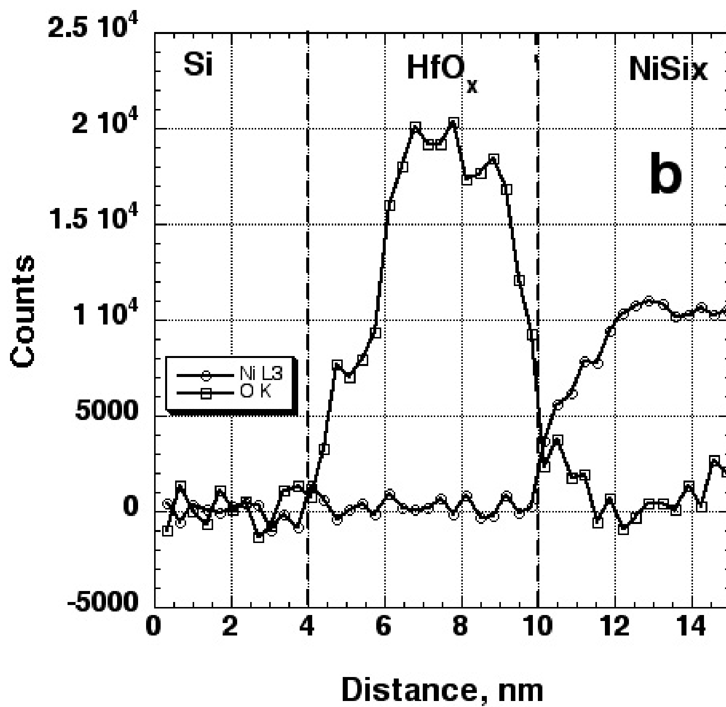

Fig. 6: (a) Dark field STEM image of FUSI gate stack. EELS spectra were taken at each point along profile in (a); Note a dark band between HfO_2 and NiSix, which is attributed to oxygen. No band is observed in Fig. 5a. (b) Elemental profiles for Ni (open circles) and oxygen (open squares).

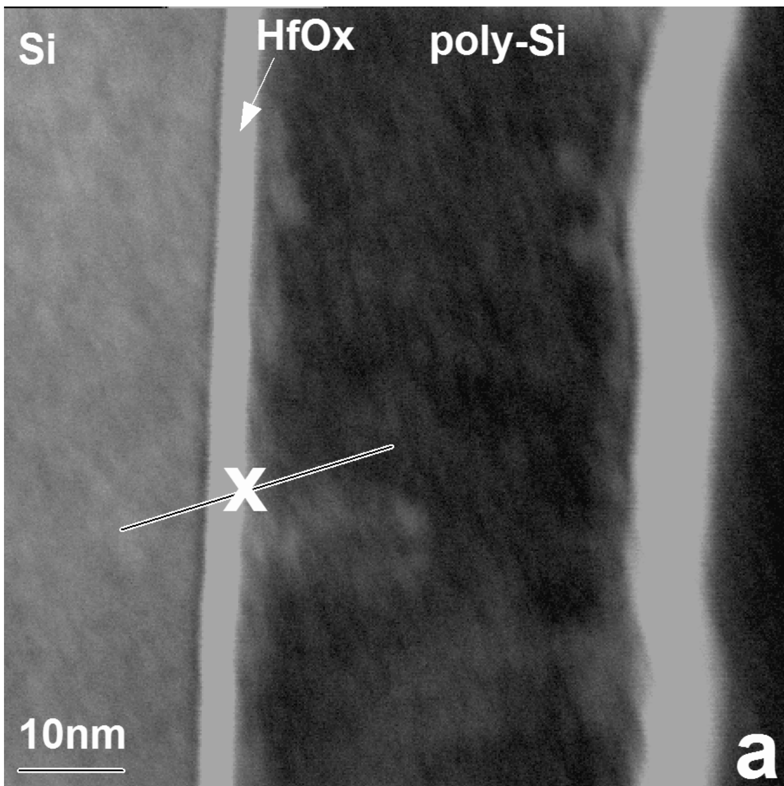

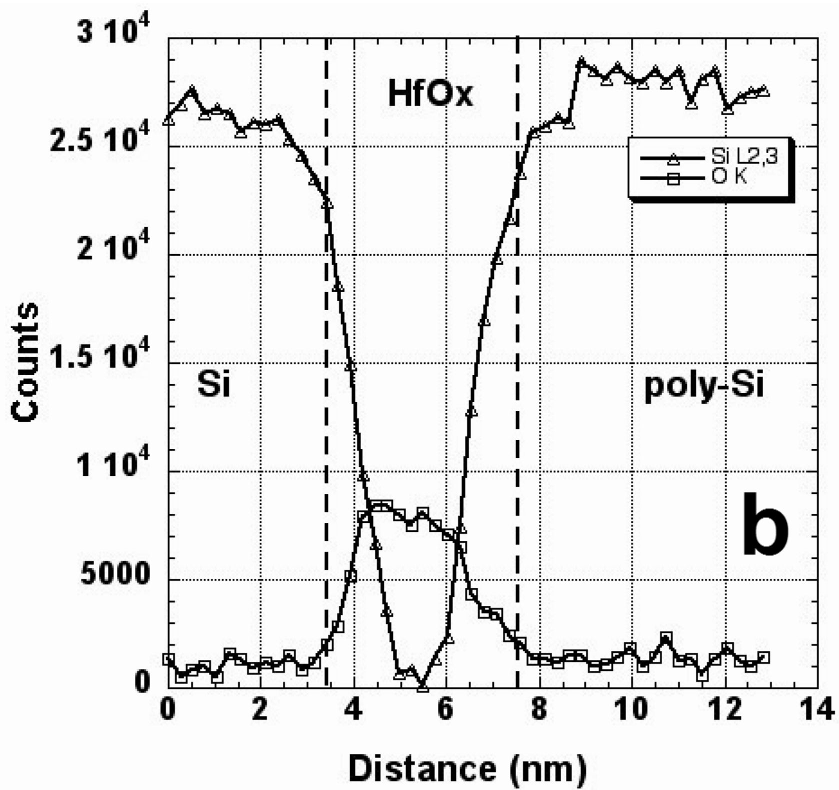

Fig. 7: Dark field STEM image (a) and EELS elemental profiles for oxygen (open squares) and Si (open triangles) (b) across Si/SiOx/HfO_2/poly-Si stack.

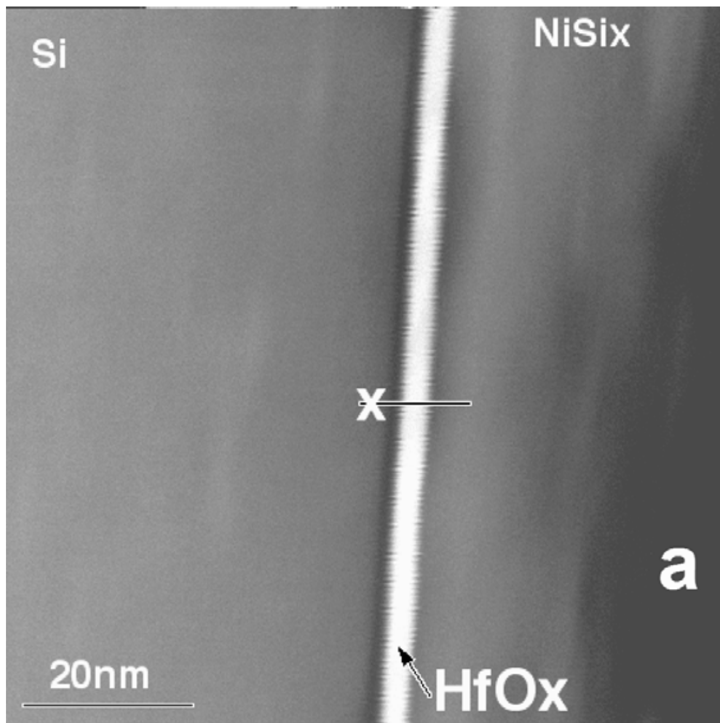

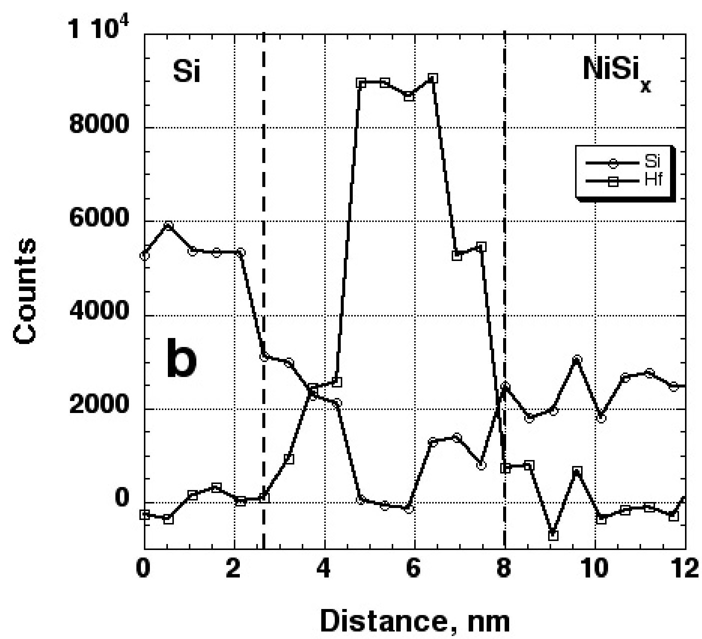

Fig. 8: (a) Dark field STEM image of FUSI gate stack. EELS spectra were taken at each point along profile in (a); (b) Elemental profiles for Hf (open squares) and Si (open circles).